2022 IEEE Symposium on VLSI Technology and Circuits (VLSI Technology and Circuits) | 978-1-6654-9772-5/22/$31.00 ©2022 IEEE | DOI: 10.1109/VLSITechnologyandCir46769.2022.9830205

A 286nW, 103V High Voltage Generator and Multiplexer for Electrostatic Actuation in Programmable Matter

Yimai Peng[1], Gordy Carichner[1], Yejoong Kim[1], Li-Yu Chen[1], Rémy Tribhout[2], Benoît Piranda[2], Julien Bourgeois[2], David Blaauw[1], Dennis Sylvester[1]

[1]University of Michigan, Ann Arbor, MI, USA, [2]FEMTO-ST Institute, Besançon, France

Abstract

We present a high-voltage-generation-and-multiplexing (HVGM) chip, specifically designed for electrostatic actuation of micro-robots. It can individually control 12 pairs of +/- electrodes using a positive and negative charge pump and mux-structure, consumes 286nW in steady state and 533nW when transitioning a 10pF electrode at 155V/s, and produces a differential voltage of 103V (29× voltage gain from 3.6V) in measurement. We also show a complete microsystem of stacked die, measuring 3×1.4×1.1mm, including HVGM, processor, radio, and harvester for energy autonomous operation.

Introduction and Proposed Approach

Improved 3D printing and MEMS technology have brought the realization of *programmable matter* [1] (PM) within reach. PM consists of tiny, mm-scale quasi-spherical robots called *Catoms*, which can autonomously attach themselves in different positions to their neighbors using electrostatic forces (Fig. 1). By combining thousands of Catoms, a morphable 3D-structure can be programmed to take arbitrary shapes. PM enables instant functional expression of new shapes and opens up a host of industrial and artistic applications.

A key challenge to electrostatic actuation in PM (and other micro-robotic applications) is the generation and control of high voltages (>100V). A high-voltage generation (HVG) chip must be contained inside the Catom, meaning: 1) Chip size should be < 3mm to ensure the Catom is small and light, precluding use of bulky off-chip components (e.g., inductors for boost converters [4]). 2) Given the small battery [10], sub-μW power is needed to ensure lifetime. 3) To allow Catoms to position themselves in different ways, multiple (~12) electrodes with individual voltage control are required. 4) Electrodes present only a capacitive load (no DC current) and at low frequencies (<100Hz) the load seen by HVG has very low reactive power (CV^2f_{sw} ≈ 100s of nW). This make achieving high efficiency challenging since power overheads (clock generation, switching loss, leakage) are not amortized over a large output current.

Prior on-chip HVGs typically employ Dickson charge pumps [2][3][6] (rather than serial-parallel multipliers [5], commonly used for AC voltage generation) but have >100uW power consumption and limited voltage gain of 10–15×. Furthermore, prior methods *directly connect the electrode to the pump* (Fig. 2). For 12 electrodes, this requires 12 separate pumps, leading to excessive size and power.

This paper proposes HVGM consisting of a *single pump with 12 novel high-voltage mux circuits* that enable individual control for each electrode output voltage (Fig. 3), amortizing area and switching overhead/leakage. Also, since the mux can turn electrodes off (0V) while keeping the pump active, we avoid discharge and recharge of flying pump capacitors, further saving significant energy. Implemented in a ~70V process, we obtain > 100V differential potential by implementing both positive and negative pumps, avoiding the need for a higher voltage (but less efficient) technology.

Circuit Implementation of HVGM

Fig. 4 shows the positive and negative pumps, generating -40V and 70V, respectively. To achieve low power, on-chip clock generation uses a leakage-based ring oscillator [9], modulated by bias voltage V_{BP}/V_{BN}. The key circuits are the 12 high voltage multiplexers (HVMUX) that select the proper positive and negative voltages from the charge pump outputs for electrostatic actuation and overcome several circuit challenges. For the positive voltage mux, HVMUX-P, Fig. 5 (top left) shows how the control signals of the pass gate $S_1 – S_m$ are level shifted [8]. Given a *PMOS* pass gate for the positive output voltage, the bodies $S_1 – S_m$ must be connected to $V_1 – V_m$, resulting in a large forward-bias diode current D_{DB} when the output voltage on P_n is larger than that on internal nodes $V_1 – V_m$. We therefore add diodes D_1 - D_m to block this current and arrange them serially to equalize their reverse bias condition, lowering the diode voltage potential and reducing their leakage to sub-pA levels.

A second challenge manifests when a voltage switch S_i (i ranges from 1 to m) ramps up the output voltage of P_n, drawing a large in-rush charge from the charge pump, collapsing V_i and other electrode voltages. Hence, the charge transfer rate from $V_1 – V_m$ to P_n must be carefully limited to guarantee stable voltages at all electrodes. We address this using switch S_P and capacitor C_P, creating an equivalent resistance modulated by S_P switch frequency. S_P is switched in a non-overlapping fashion with S_i to avoid a direct path from V_i to P_n until P_n has stabilized. The control signal for S_P is also level shifted. Since V_{SMP} on C_P changes rapidly during a charge transfer cycle, it cannot be tracked by a level shifter. We therefore implemented S_P with an *NMOS* transistor and its control signal is level shifted relative to V_{Pn}, which is slow and can be tracked. For similar reasons $S_1 – S_m$ are implemented with PMOS transistors and their control signals level shifted from V_i.

A third challenge is that, with the addition of diodes $D_1 – D_m$, the pump can only pull the output voltage P_n up. With no DC load current, the voltage on P_n will decrease extremely slowly through leakage. Hence, we implement an intentional discharge path, with switch-cap resistor S_{D1}, S_{D2}, and C_D. By using the regular supply voltage to control switches S_{D1} and S_{D2}, we limit charge transfer to $C_D(V_{DD}\text{-}Vth)$ per cycle, and discharge P_n gradually. When not discharging, both S_{D1} and S_{D2} are off, creating a stack effect to strongly reduce leakage.

Using the same approach for the negative charge pump, HVMUX-N, switches S_p, S_{D1}, and S_{D2} would need to be *PMOS*, which is not possible since their n-well, connected to the negative voltage N_n, would short to P_{sub} through the well diode. We instead opt for a simpler binary mux that selects between V_n and GND (Fig. 4 bot, right). In this mux, the level shifter for S_n is referenced to V_n since it is the stable voltage. Charge transfer between V_n and N_n is limited by poly resistor R_n. When S_n is disabled, the source voltage of S_n is $V_{s,Sn} = V_n$ while $V_{d,Sn} = N_n = 0V$. When S_n is then enabled, the level shifter applies a gate voltage $V_{g,Sn} = V_n\text{-}V_{DD}$ and the source voltage of S_n will rapidly rise to $V_n\text{-}(V_{DD}\text{-}Vth)$, turning the switch off and *self-limiting* the charge transfer. $V_{s,Sn}$ will then slowly drop as charge flows out through R_n, re-enabling S_n and transferring charge from N_n to V_n in a controlled fashion. HVMUX-N provides a coarse differential voltage selection of ~40V while HVMUX-P provides fine grain control with a step of ~3V. To allow an application-dependent value of V_N it is determined by a hard-wired connection between the negative pump output (V_{-1} to V_{-13}) and V_n using a wirebond.

Measurement Results

HVGM is fabricated in 180nm HVBCD and occupies 3.67mm^2, including 24 electrode pads. Fig. 6 shows a fully functional integrated micro-system to be placed inside a Catom, consisting of 8 stacked die including a PV cell for energy harvesting and a 22.8uWh battery. Fig. 7 shows the measured positive and negative electrode transition with different power settings. At V_{DD} = 3.6V and F_{clock} = 625Hz, HVGM generates a differential voltage of 103V, for a voltage gain of 29×. In this case, it consumes 286nW in steady state (i.e., no electrode transitioning) and 533nW when charging a 10pF electrode at 155V/s, which is sufficient for PM to achieve a 0.2Hz periodic actuation. HVGM can support a 60Hz actuation by increasing its frequency to 46kHz, consuming 14.1μW power, or it can further lower its power to 130nW to sustain a DC voltage of ~100V on the electrodes.

Figs. 8 and 9 shows measured maximum electrode voltage as a function of V_{DD} and slew rate across clock frequencies. Fig. 10 shows the average power per electrode for a varying number of transitioning electrode pairs. There is significant amortization of fixed power at higher electrode counts, confirming the benefits of a single pump topology. Fig. 11 shows the programmable voltage output for the positive electrodes. Table I compares HVGM with prior work, showing the highest voltage gain and lowest power consumption to generate high voltages for programmable matter and micro-robots.

References

[1] B. Piranda et al., Auto. Robot 2018. [2] M. Marx et al., JSSC, 2019.
[3] Y. Ismail et al., ISSCC, 2014. [4] M. Lok et al., TPEL, 2016.
[5] Beaulieu et al., ISCAS16. [6] M. E. Karagozler et al., ISCAS, 2011.
[7] S. Dai et al., TCAS1, 2015. [8] Z. Liu et al., CICC, 2013.
[9] I. Lee et al., JSSC, 2016. [10] M. Fojtik et al., JSSC, 2013.

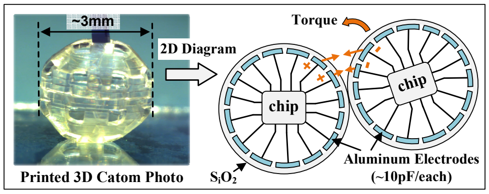

Fig. 1. Photo for a fabricated programmable matter Catom (left) and conceptual diagram showing actuation with electrostatic force (right).

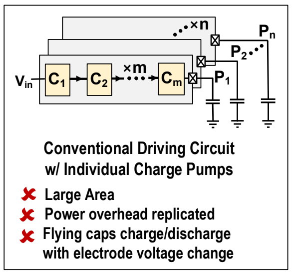

Fig. 2. Diagram of a conventional HVG.

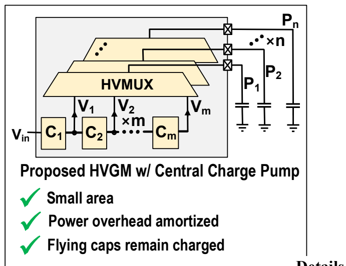

Fig. 3. Diagram of proposed HVGM.

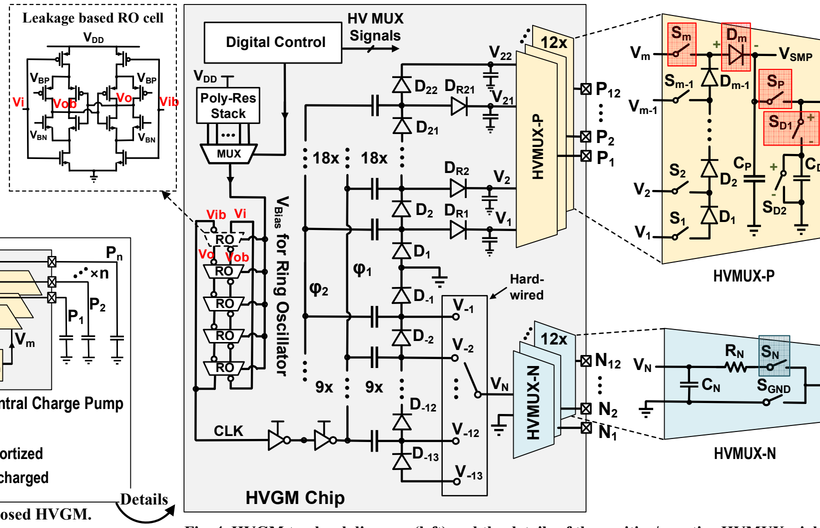

Fig. 4. HVGM top level diagram (left) and the details of the positive/negative HVMUX right).

Table. 1. Comparison with prior HVG works with no/light load conditions.

	This work	[2] JSSC'19	[3] ISSCC'14	[6] ISCAS'11	[7] TCAS1'15	[5] ISCAS'16
Technology	0.18µm	0.35µm	65nm	1µm	0.8µm	0.8µm
Topology	Charge Pump + Multiplexer	Charge Pump	Charge Pump	Rectifier+ Charge Pump	HV Amp+ Multiplexer	Voltage Doubler
Input voltage	3.6V	3.3V	2.75V	5V	5V (LV) 300V (HV)	15V
Output Voltage	103 V	32.6 V	34 V	33 V	290 V	360.5 V
Voltage Gain	28.6	9.9	12.3	6.6	58/0.97	24.0
Output Voltage Frequency Range	DC – 60Hz	DC	DC	DC – 500Hz *	DC	DC – 60Hz
Power Consumption	130nW @ DC 286nW @0.2Hz 14.1µW@ 60Hz	97µW @ DC	Not Reported**	Not Reported**	90mW @ DC	Not Reported**
Load Capacitance	10pF	-	-	10 pF	10 nF	-
Fully integrated	Yes	Yes	Yes	Yes	Yes	Yes
Adjustable Output	Yes	No	No	Yes	Yes	Yes
# of Output Port	12	1	1	1	1	1

* Estimated with the measured voltage slew rate.
** These works are not power constrained so no power is reported.

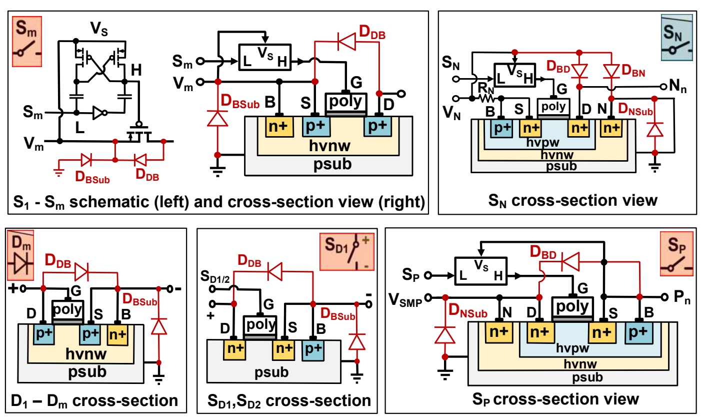

Fig. 5. The HVMUX implementation with switches/diodes and their cross-section views (bottom).

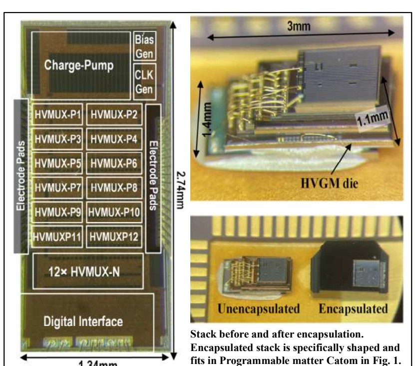

Fig. 6. Photo showing the HVGM die and the full-stack system consisting HVGM, battery, radio, processor and energy harvesting die.

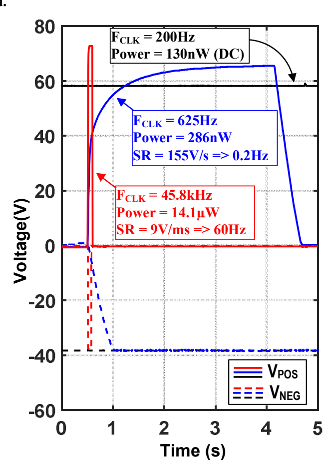

Fig. 7. Measured transient waveform showing voltage transition of the HVGM electrodes.

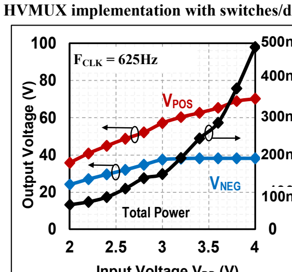

Fig. 8. Measured max voltage with V_{DD}.

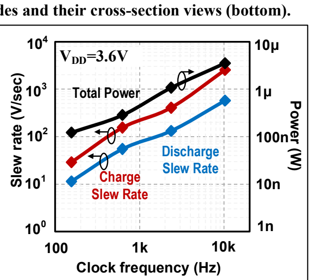

Fig. 9. Measured HVGM Slew rate with mux frequency.

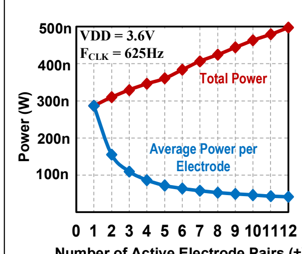

Fig. 10. Measured HVGM power with the number of active electrode.

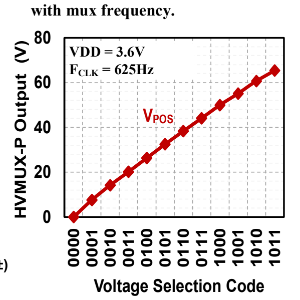

Fig. 11. HVGM programmable output.